

Article

## Optimal Passive Dynamics for Physical Interaction: Catching a Mass

Kevin Kemper<sup>1</sup>, Hamid Reza Vejdani<sup>2,\*</sup>, Brent Piercy<sup>3</sup> and Jonathan Hurst<sup>2</sup>

<sup>1</sup> Meka Robotics, 255 Potrero Ave, San Francisco, CA 94103, USA; E-Mail: kkemper@gmail.com

<sup>2</sup> Dynamic Robotics Laboratory, Department of Mechanical Engineering, Oregon State University, Corvallis, OR 97331, USA; E-Mail: jonathan.hurst@oregonstate.edu

<sup>3</sup> Ekso Bionics, 1414 Harbour Way South Suite 1201, Richmond, CA 94804, USA; E-Mail: bptheincredible@gmail.com

\* Author to whom correspondence should be addressed; E-Mail: hrvn@enr.oregonstate.edu; Tel.: +1-541-737-4807; Fax: +1-541-737-2600.

Received: 4 March 2013; in revised form: 12 April 2013 / Accepted: 22 April 2013 /

Published: 2 May 2013

---

**Abstract:** For manipulation tasks in uncertain environments, intentionally designed series impedance in mechanical systems can provide significant benefits that cannot be achieved in software. Traditionally, the design of actuated systems revolves around sizing torques, speeds, and control strategies without considering the system's passive dynamics. However, the passive dynamics of the mechanical system, including inertia, stiffness, and damping along with other parameters such as torque and stroke limits often impose performance limitations that cannot be overcome with software control. In this paper, we develop relationships between an actuator's passive dynamics and the resulting performance for the purpose of better understanding how to tune the passive dynamics for catching an unexpected object. We use a mathematically optimal controller subject to force limitations to stop the incoming object without breaking contact and bouncing. The use of an optimal controller is important so that our results directly reflect the physical system's performance. We analytically calculate the maximum velocity that can be caught by a realistic actuator with limitations such as force and stroke limits. The results show that in order to maximize the velocity of an object that can be caught without exceeding the actuator's torque and stroke limits, a soft spring along with a strong damper will be desired.

**Keywords:** passive dynamics; impedance; catching

---

## 1. Introduction

Robots excel at precise position control and are useful for tasks that make use of this ability, such as traditional industrial robots. However, physical interaction tasks such as catching a ball, walking, running, grasping unknown objects, constrained contact and even simple force or torque control have historically been difficult for robots. Each of these tasks involves dynamic effects such as unexpected impacts and/or a significant transfer of kinetic energy between the robot and its environment. Animals far outperform robots at many of these tasks, and we believe that the robot's poor performance relative to animals is due to inherent mechanical limitations (such as high inertia and improperly chosen impedance) in traditional robotic mechanisms.

Consider a traditional industrial robot arm, powered by electric motors with large gear reductions and rigid links. The traditional approach to catching an object is to rely on complex vision systems to estimate the trajectory of the object and carefully match the velocity at the time of contact to avoid large impact forces [1]. Because these systems require an enormous amount of information about the object prior to contact, these methods are not robust or practical for systems outside of a controlled setting. Any error in these calculations can cause very large impact forces, possibly damaging the robot. In the extreme case where no information is known about the object prior to contact, the system must rely completely on software control and the mechanics of the actuator to determine the response. However, when the system impacts an unseen object in the environment, the motor's inertia must be accelerated through the transmission. If there is a gear reduction between the motor and the linkage, the motor's inertia as seen by the object is multiplied by the square of the gear reduction. The sudden acceleration of this "reflected" inertia causes very large force spikes; these passive dynamics cannot be overcome using software control alone. If an object impacts the arm, such as a baseball, the arm will behave as a rigid inertial object and the software control will have no part in its dynamic response.

Passive dynamics are not always harmful. As an example of passive dynamics improving performance, a mechanical spring in series with a motor can reduce force error in response to large position disturbances, as exemplified by a fishing rod. The flexibility of the rod allows the fisherman to maintain a steady force on the line, eliminating force spikes that would snap the fishing line. However, this improvement applies only to the specific case of maintaining a constant force and its robustness to position disturbances; a series spring will reduce the performance of the system for position control [2]. For peak performance in a robotic system, the passive dynamics must be tailored to the specific task. This is roughly analogous to impedance matching in electrical systems.

In this paper we define how an actuator's passive dynamics affect performance when experiencing an unexpected impact such as catching an object (Figure 1). We lay out a mathematical framework for realistic mechanical systems that includes a motor with torque limits and inertia, a series spring and a series damper, as shown in Figure 2.

**Figure 1.** Given a system’s characteristics such as torque limits, displacement, and inertias, there exists an optimal passive element that, when used in series, will increase the system’s performance when catching an object.

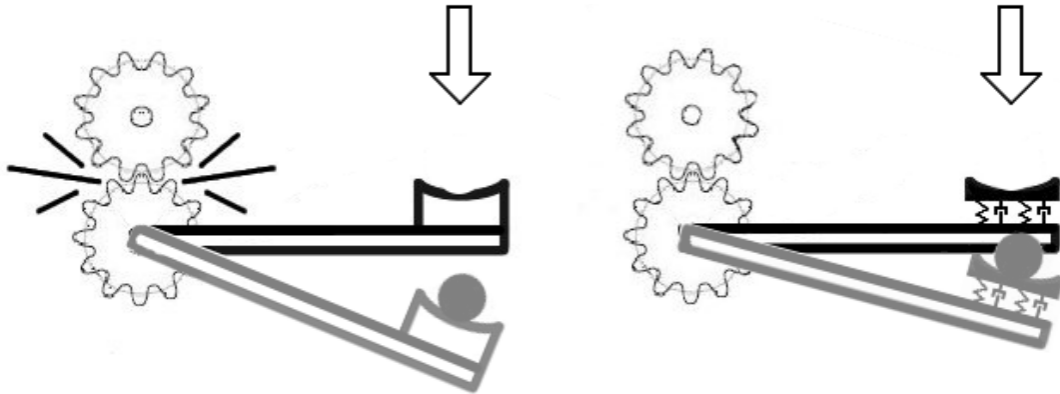
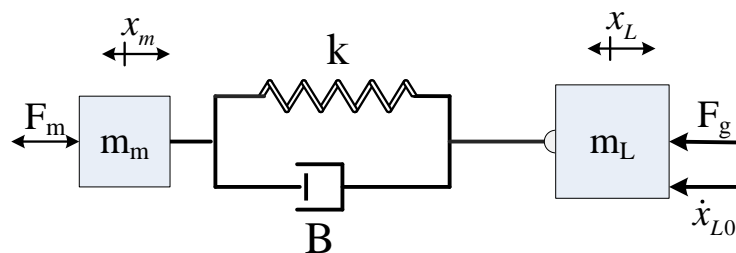


**Figure 2.** System schematic. The motor inertia is represented as a mass ( $m_m$ ) with gravity ( $F_g$ ) only acting on the load mass ( $m_L$ ). This is analogous to an electric motor attached to a ball screw transmission where the rotational inertia is much greater than the mass of the transmission itself. The load mass has initial velocity ( $\dot{x}_{L0} = v_0$ ) at  $t = 0$ .



In order to keep the problem well defined, we specify that the goal of the actuator is to stop a mass moving relative to the actuator given some initial velocity without allowing it to bounce. Examples of these tasks include but are not limited to docking a spacecraft, catching an object with limited peak forces, landing on an uncertain ground with a legged robot, or minimizing head impact trauma in a human/robot environment. We then describe the mathematically optimal passive dynamics required to achieve the best possible response, based on fundamental physical limits. These results will enable designs of mechanical systems that will be well suited for catching task, especially involving spring-like behavior.

## 2. Background

Muscular systems in animals incorporate elastic elements, which are most often examined while investigating locomotion, and are generally discussed in the context of energy storage [3–5]. Roboticists have built machines designed to mimic this spring-like behavior [6–9]. Although the designers of these running machines acknowledge that elasticity provides robustness, their studies generally focus on energy storage and efficiency. We wish to examine in more detail how these passive elements contribute to general force control and manipulation with the environment.

Discussions into how actuators behave when moving from free motion to a constrained contact (an impact) often focus on how to develop controllers to remove energy from the impact [10–12]. In most cases the authors acknowledge that the controllers are limited by the delay caused by the intrinsic mass and inertia even with instantaneous physical collision detection. They avoid this issue by limiting the investigation to contact with soft, compliant types of surfaces [12] or rely on intrinsic (and uncharacterized) mechanical compliance in the design [11].

Investigations into force control found that series compliance in an actuator can increase stability, and in some cases is required for stable operation [13–17]. Researchers at the Massachusetts Institute of Technology (MIT) Leg Laboratory explored these ideas and created the Series Elastic Actuator (SEA). The MIT-SEA is designed specifically to include an elastic element as a force sensor and low impedance coupling between the drive system and the load to improve force control. It has been shown that this configuration provides mechanical filtering to handle shock loads and increases the bandwidth for force control [18,19]. The MIT-SEA offers great advantages when considering force control, however, there has been no formal study of the performance on impacts such as catching unknown objects. Further work to improve the MIT-SEA has focused on control architecture, e.g., [20,21] or transmission design (e.g., [22–24]). Buerger *et al.* [25] presents a loop shaping design method for the design of the actuator controllers for physically interactive machines. They redefined stability and performance and introduced a measure of complementary stability. They showed that their control strategy works well on real robots.

An extension of MIT-SEA has been proposed by Hurst *et al.* [26]. They concluded that the added damping provides higher bandwidth than a purely series-elastic element and reduces unwanted oscillations in specific situations. Initial force spikes observed by the drive system at impact are greater than would be observed by just an elastic element, but are vastly improved compared with a fully rigid system.

In this work we derived mathematical formulas for the design of the passive elements of the catching system. Previous studies investigated this problem numerically and there is not any closed form formulas for this problem. The closed form formulas in this work helps the designer to understand the effect and sensitivity of the actuator parameters on the behavior of the system. This paper builds on our previous investigation into how the passive dynamics of the physical system contribute to the performance of an actuator in “constrained contact” tasks [2]. In that earlier work, we described two actuation scenarios, position control and force control, and derived the relationship between physical damping and stiffness to the respective goals. We concluded that for an actuator to perform well at maintaining a constant force on a moving object, low system impedance is needed, while a higher impedance is needed to obtain high performance position control. For a system to perform well at both of these tasks, variable impedance is necessary.

### 3. Problem Domain

There are several performance metrics for a catching system. These include the maximum initial velocity given a particular load mass that can be stopped, the peak force experienced by the load, the torque required by the motor, and the stroke length needed to dissipate the relative kinetic energy. Depending on the design of the system, certain aspects of the design may be fixed. One example of a

stroke and force limited actuator is a hydraulic cylinder. These fixed parameters affect the optimal spring and damper that could allow this system to catch a particular mass at an unknown velocity.

To develop the relationships between an actuator's design parameters, we investigate the series elastic/damping actuator (SEDA) in Figure 2. Our actuator includes damping and elasticity because they are both inherent in a physical system and possibly useful in decoupling the inertias to help us minimize peak forces. We want to know how to select these elements ( $k$  and  $B$ ) to design the best possible actuator for a catching task.

In this paper, we define relationships between series stiffness, series damping, drive system inertia and the drive system torque limits in a specific theoretical scenario. To simplify the discussion, we use "motor" to describe the drive system as a whole—transmission and motor characteristics. The following symbols in Table 1 describe our model:

**Table 1.** Symbols for mathematical formulas and simulation.

| Symbol      | Description                          | Unit                  |
|-------------|--------------------------------------|-----------------------|
| $x_L$       | Load position                        | $m$                   |
| $x_m$       | Motor position                       | $m$                   |
| $z_1$       | Rigid body motion of two masses      | $m$                   |
| $z_2$       | Relative motion of two masses        | $m$                   |
| $k$         | Spring constant                      | $N \cdot m$           |
| $B$         | Damping constant                     | $\frac{N \cdot s}{m}$ |
| $g$         | Acceleration of gravity              | $\frac{m}{s^2}$       |
| $m_m$       | Motor/transmission mass              | $kg$                  |
| $m_L$       | Load mass                            | $kg$                  |
| $F_m$       | Motor force                          | $N$                   |
| $F_{limit}$ | Motor force limit                    | $N$                   |
| $F_g$       | Force due to gravity                 | $N$                   |
| $F_d$       | Force caused by the dynamic elements | $N$                   |
| $v_0$       | Load initial velocity                | $\frac{m}{s}$         |

In addition to the reactive elements  $k$  and  $B$ , we include motor force limits as well as motor inertia (represented as the mass  $m_m$ ). If infinite force were possible, there would be no requirements for designing the impedance of the actuator. In other words, it would not matter how soft or stiff the elements were, so long as the motor and load are kinematically linked. Likewise, if we have zero motor mass, we do not need to be concerned with the values of  $k$  and  $B$  since our motor could instantaneously move to provide the required force. These ideal cases, while highly desired, are not physically possible. In realistic systems there are limits to the actuator's force, stroke length, and inertia.

#### 4. System Model

Our series impedance actuator model, shown in Figure 2, is entirely linear with gravity only acting on the load. The model is analogous to an electric motor attached to a ball screw transmission where

the rotational inertia is much greater than the mass of the transmission itself. We start by defining the differential equations that describe the motion of the system:

$$[m] \begin{Bmatrix} \ddot{x}_L \\ \ddot{x}_m \end{Bmatrix} + [B] \begin{Bmatrix} \dot{x}_L \\ \dot{x}_m \end{Bmatrix} + [k] \begin{Bmatrix} x_L \\ x_m \end{Bmatrix} = \begin{Bmatrix} m_L g \\ F_m(t) \end{Bmatrix} \tag{1}$$

where

$$[B] = \begin{bmatrix} B & -B \\ -B & B \end{bmatrix} \tag{2}$$

$$[k] = \begin{bmatrix} k & -k \\ -k & k \end{bmatrix} \tag{3}$$

$$[m] = \begin{bmatrix} m_L & 0 \\ 0 & m_m \end{bmatrix} \tag{4}$$

We define the performance of the system as the largest possible  $v_0$  that the system can encounter without bouncing the incoming load, given a motor torque limit. Because of this limit and the objective function (velocity) that we have here, the problem cannot be expressed within the framework of classical optimal control theory (e.g., LQR).

In order to calculate the maximum  $v_0$  the actuator can handle, we decouple (1) into two independent single degree of freedom (SDOF) systems, which will isolate the relative motion and the global movement in the system. Since the mode shapes are perpendicular to each other with respect to the mass, stiffness and damping matrices:

$$\{\phi\}_i^T [m] \{\phi\}_j = 0, \quad i \neq j \tag{5}$$

$$\{\phi\}_i^T [k] \{\phi\}_j = 0, \quad i \neq j \tag{6}$$

$$\{\phi\}_i^T [B] \{\phi\}_j = 0, \quad i \neq j \tag{7}$$

we have

$$\begin{Bmatrix} x_L \\ x_m \end{Bmatrix} = \{\phi\}_1 z_1(t) + \{\phi\}_2 z_2(t) \tag{8}$$

This allows us to decouple the system by pre-multiplying both sides by  $\{\phi\}_i^T$ . The vectors  $\{\phi\}_1$  and  $\{\phi\}_2$  are the mode shapes of the system. We then can write a new set of equations describing the decoupled system as

$$(m_L + m_m) \ddot{z}_1(t) = m_L g + F_m(t) \tag{9}$$

$$m_e \ddot{z}_2(t) + B_e \dot{z}_2(t) + k_e z_2(t) = m_L g - \mu F_m(t) \tag{10}$$

where the equivalent parameters are

$$m_e = m_L (1 + \mu) \tag{11}$$

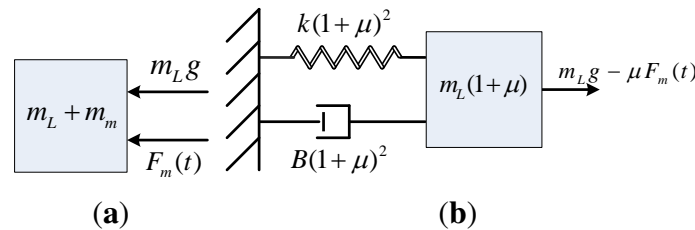
$$B_e = B (1 + \mu)^2 \tag{12}$$

$$k_e = k (1 + \mu)^2 \tag{13}$$

$$\mu = \frac{m_L}{m_m} \tag{14}$$

Equations (9) and (10) can be described in Figure 3(a) and Figure 3(b) respectively.

**Figure 3.** The original system in Figure 2 can be broken into two separate single degree of freedom systems. Figure 3(a) and Figure 3(b) illustrate a physical representation of the new systems. The rigid body motion describes how the masses move together and the relative motion shows how the two masses move relative to each other. (a) The rigid body motion of the system; (b) Relative motion of the masses.



The two new models demonstrated in Figure 3 are the two independent behaviors exhibited by the system. Figure 3(a) represents the rigid body motion of the system and describes how the masses move together. Figure 3(b) describes the oscillation of the masses relative to each other.

The boundary conditions for the initial system are

$$\begin{Bmatrix} x_L \\ x_m \end{Bmatrix}_{t=0} = \begin{bmatrix} 0 \\ 0 \end{bmatrix}, \quad \begin{Bmatrix} \dot{x}_L \\ \dot{x}_m \end{Bmatrix}_{t=0} = \begin{bmatrix} v_0 \\ 0 \end{bmatrix} \tag{15}$$

then the initial conditions for the new system become

$$z_1(0) = 0 \tag{16}$$

$$\dot{z}_1(0) = \frac{\mu v_0}{1 + \mu} \tag{17}$$

$$z_2(0) = 0 \tag{18}$$

$$\dot{z}_2(0) = \frac{v_0}{1 + \mu} \tag{19}$$

The force generated by the dynamics is defined as

$$F_d(t) = B(\dot{x}_m - \dot{x}_L) + k(x_m - x_L) \tag{20}$$

This can be written in the new SDOF coordinate system by substituting Equation (8) into Equation (20):

$$F_d(t) = -B(1 + \mu)\dot{z}_2(t) - k(1 + \mu)z_2(t) \tag{21}$$

Equation (21) can be interpreted as the reaction force in Figure 3(b) if the dynamics of the system is divided by  $(1 + \mu)$ .

$$m_L \ddot{z}_2 + B(1 + \mu)\dot{z}_2 + k(1 + \mu)z_2 = \frac{m_L g}{1 + \mu} - \frac{\mu F_m}{1 + \mu} \tag{22}$$

To keep the dynamic force ( $F_d(t)$ ) always negative (the spring in compression), the support reaction in the equivalent SDOF has to be positive (or in tension) because of the minus sign in Equation (21).

### 5. Controller

Because we are interested in determining the influence of the passive dynamics and physical limitations of the system, we must develop controllers that are optimal for each specific configuration of system parameters. The optimal controller can most easily be understood from the perspective of the SDOF system in Figure 3(b), which represents the relative motion of the two masses in our original system (Figure 2). The differential equation of this system was represented in Equations (10–14). The most important goal is to prevent the load from bouncing away from the actuator—therefore, the force applied relative to each other must remain positive, keeping the spring compressed. Immediately after impact, the equivalent object (object in Figure 3(b)) is compressing the spring ( $\dot{z}_2 < 0$ ). The optimal control strategy is to slow this motion down and immediately begin removing energy from the system. For this purpose, the maximum motor force should be applied in the opposite direction of the load movement to apply the largest negative work to the system (Figure 4(a)). Therefore, the differential equation would be Equation (23). When the velocity of the equivalent object reaches zero and switches direction, which is equivalent to the time that the relative velocity of our two original masses becomes zero and switches direction,  $\dot{z}_2 = 0$  in Equation (23), the motor force should also switch direction and continue to remove energy from the system. In this case, since the load is moving back and decompressing the spring (Figure 4(b)), for the maximum motor force to be applied in the opposite direction of the load movement, the maximum force should be applied towards the left (Figure 4(b)), and hence the differential equation of the system would be Equation (24). If the motor can remove sufficient energy to prevent the load from bouncing away, the catch is successful. By following this strategy, the largest possible initial velocity can be caught by the actuator given its physical limitations.

$$m_e \ddot{z}_2(t) + B_e \dot{z}_2(t) + k_e z_2(t) = m_L g + \mu F_{limit} \quad \text{when } \dot{z}_2 < 0 \quad (23)$$

$$m_e \ddot{z}_2(t) + B_e \dot{z}_2(t) + k_e z_2(t) = m_L g - \mu F_{limit} \quad \text{when } \dot{z}_2 > 0 \quad (24)$$

**Figure 4.** The first two phases of the controller. After these two phases, the load has been caught and simple position control can move the load to the desired position. The gray drawings show the past status and the moving direction of the mass is shown by the velocity vector underneath the mass. (a) First stage of the controller. The equivalent mass initially moves toward the right with the controller pushing into the mass (spring is being compressed); (b) Second stage of the controller. When the equivalent mass begins to move back toward the initial position, the controller pulls on the mass to the right (spring is being decompressed).

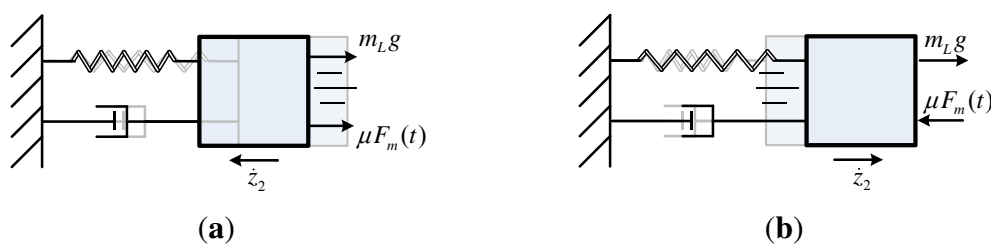
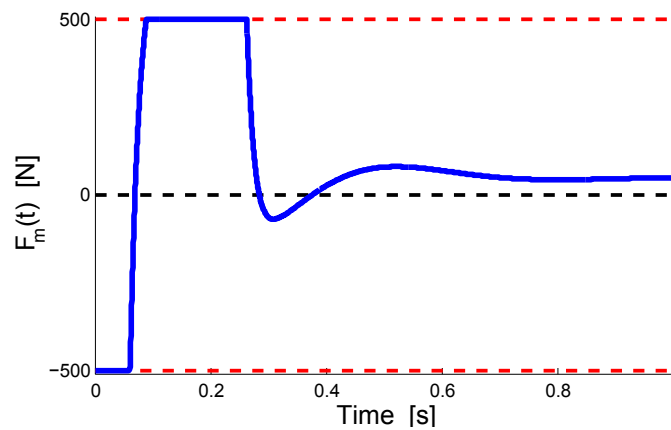


Figure 5 shows an example of the input force produced by the controller. The upper and lower boundaries of this force profile depict the ultimate capacity of the system to catch the load mass and the intervals can be obtained using Equations (9, 10, 21). For our real system this is interpreted as applying the maximum force in the direction of gravity initially then applying the maximum force upward. The mass will not bounce if the actuator and damper are able to dissipate the whole initial velocity before the mass crosses the zero position.

**Figure 5.** An example of the input force profile generated by the controller. In this case, the motor limit,  $F_{limit}$ , is 500 N and the motor mass and load mass are  $m_m = m_L = 10\text{ kg}$ .



### 6. Undamped Actuator: Analytical Derivation

For a special case of a system without damping, the relation between the maximum possible initial velocity and maximum motor force as well as other mechanical properties of the system can be found by dissipating all of the kinetic energy of the system with the motor force:

$$\frac{1}{2}m_L \left( \frac{v_0}{1 + \mu} \right)^2 = 2 \frac{\mu}{1 + \mu} F_{limit} z_{2limit} \tag{25}$$

where  $z_{2limit}$  is the maximum spring deflection. Solving Equation (22) for the maximum  $z_2$  with zero damping yields:

$$z_{2limit} = \frac{1}{1 + \mu} \left( \frac{F_{eq}}{k(1 + \mu)} + \sqrt{\left( \frac{v_0}{\omega} \right)^2 + \left( \frac{F_{eq}}{k(1 + \mu)} \right)^2} \right) \tag{26}$$

where  $\omega$  is the frequency of the equivalent SDOF system and  $F_{eq}$  is the equivalent force from Figure 3b:

$$\omega = \sqrt{\frac{k(1 + \mu)}{m_L}} \tag{27}$$

$$F_{eq} = m_L g - \mu F_{limit} \tag{28}$$

After some simplification of Equation (25) with Equation (27) and Equation (28), the maximum velocity that can be caught by a non-damped system can be obtained as:

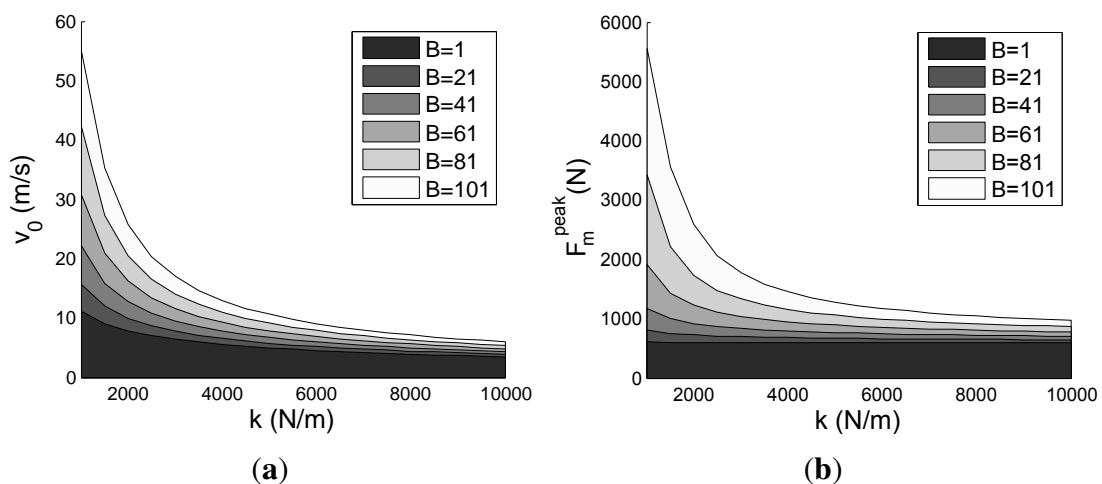
$$v_0 = \sqrt{\frac{8F_{limit} \left( m_L g + \frac{m_L}{m_m} F_{limit} \right)}{k(m_L + m_m)}} \tag{29}$$

Solving Equation (29) for  $F_{limit}$ , we can find the minimum motor force limit required to catch a mass with initial velocity  $v_0$ :

$$F_{limit} = \frac{\sqrt{(8m_L g)^2 + 32km_L(1 + \mu)v_0^2} - 8m_L g}{16\mu} \tag{30}$$

If the above force ( $F_{limit}$ ) cannot be provided, at least some damping will be required to catch the load. This can be observed in Figure 6(a) where, if the system design requires  $v_0$  of at most  $20 \frac{m}{s}$  then for  $k = 2000 \frac{N}{m}$  we at least need damping greater than about  $40 \frac{N \cdot s}{m}$  to stop the load without bouncing.

**Figure 6.** Performance of the series elastic/damped actuator while successfully stopping the load without bouncing. In each case, increasing the damping has a larger effect on the performance for softer springs. Overall performance decreasing as stiffness increases. For each figure,  $m_m = m_L = 10 \text{ kg}$  and  $F_{limit} = \pm 500 \text{ N}$ . (a) shows that increasing the stiffness decreases the maximum incoming velocity that the actuator can catch. In (b), the maximum peak force applied to a load with initial  $v_0$  is depicted. (a) Maximum  $v_0$  vs. series elasticity,  $k$ ; (b) Maximum peak force.

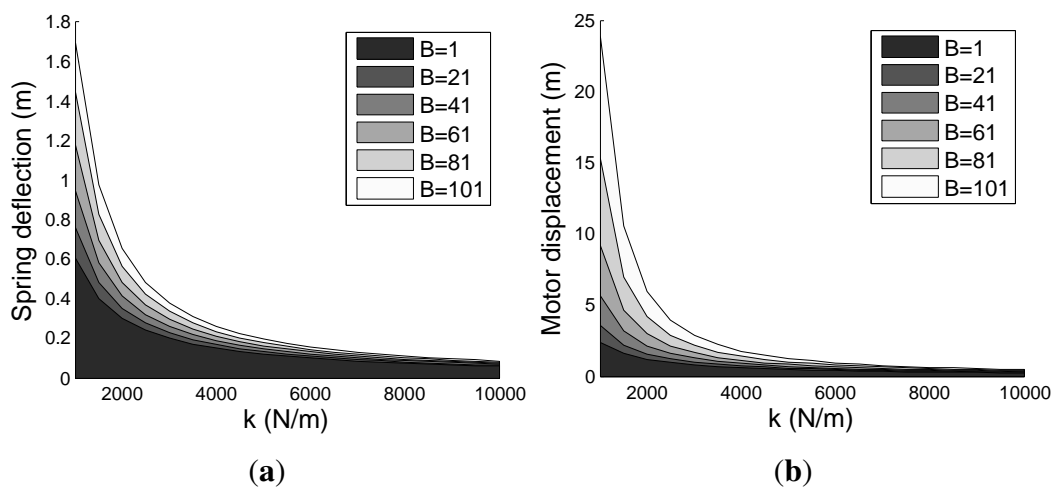


### 7. Results

Our research shows that by using a softer spring coupled with a large damper, the system greatly outperforms a rigid system at catching a high velocity load without bouncing. Figure 6(a) shows how damping and stiffness affect the maximum velocity that can be caught. We can conclude that the softer the spring, the larger the maximum initial velocity the system can catch without hitting the maximum allowable peak force. However, it is often not plausible to use a very soft spring because of inherent physical limitations like the spring deflection and actuator displacement. An interesting note is that the effect of damping on softer springs is much more significant than on stiffer springs.

To create the required design graphs (presented in Figures 6 and 7) for a general damped system, the two independent differential Equations (9) and (10) should be solved based on the discussion about the maximum motor force we had in Section 5. The moment that the dynamic force in Equation (21) becomes positive is the time that the mass loses the contact with the actuator, and it means the actuator cannot catch the load with that initial velocity. Therefore, the maximum initial velocity that the actuator is able to catch without bouncing (Figure 6(a)) is the maximum initial velocity ( $v_0$ ) in Equations (15)-(19) that keeps the dynamic force always negative. All other desired values can be obtained from  $z_1$  and  $z_2$ . For example, the distance that the motor travelled is  $z_1$  and the spring length is the same as  $z_2$ . For the maximum force applied to the actuator from the mass (or vice versa) Equation (21) (the dynamic force) can be used.

**Figure 7.** Performance of the series elastic/damped actuator while successfully stopping the load without bouncing. For each figure,  $m_m = m_L = 10\text{ kg}$  and  $F_{limit} = \pm 500\text{ N}$ . (a) shows the minimum spring length required to catch the load with the maximum possible velocity. As the stiffness increases, the required length decreases. In (b) the minimum motor travel required to catch the load is depicted. It shows that to stop the maximum velocity, the system should be very soft and the motor must be allowed to travel very far. (a) The minimum required spring length; (b) The minimum required motor distance.



An important issue is the peak force that can be safely applied to the load by the actuator. One way to use this design constraint is to begin by looking at Figure 6(b). For the maximum force that can be applied, the sets of  $k$  and  $B$  values that keep the force below the threshold should be considered. Using these values for  $k$  and  $B$ , the maximum velocity that can be caught can be found using Figure 6(a).

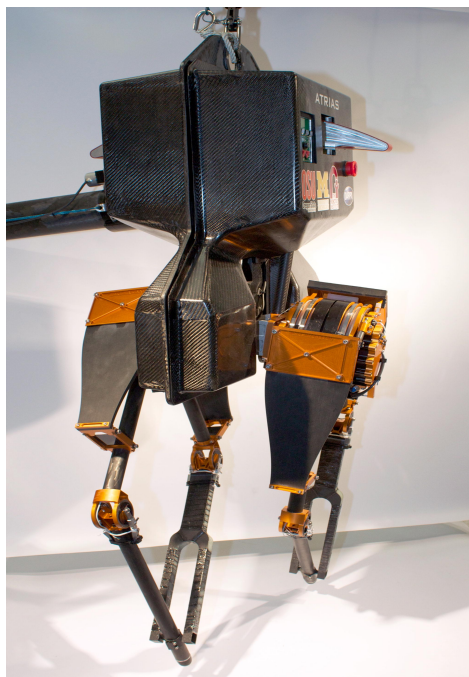
In Figure 7(a), the effect of stiffness and damping on the maximum deflection of the spring is demonstrated. For stiff systems, adding damping has little effect on the maximum displacement of the spring. Because the spring deflection is one of the inherent physical properties of the mechanism, this constraint is a useful starting point for beginning the design process. For example, for a spring deflection limit around 20 cm, no stiffness less than  $3000 \frac{N}{m}$  can be considered for catching the largest possible velocity shown in Figure 6a. If both stiffness and displacement are fixed then the motor force limit must increase or the motor mass/inertia must change.

Maximum actuator motion is another physical limitation. The graph in Figure 7(b) shows the peak motor displacement with respect to damping and stiffness of the system. For a maximum motor translation of around 50 cm, the spring should be at least as stiff as  $4700 \frac{N}{m}$  to catch the largest possible velocity.

## 8. Conclusions and Future Work

In this paper, we separated the two degrees of freedom of a series impedance actuator catching a mass into two single-DOF systems that could be more easily analyzed and controlled. The results describing the influence of stiffness, damping, and motor limitations on performance in catching an object of unknown mass and speed are intuitive; the contribution of this paper is the analytical treatment. By following the procedure outlined in this paper, engineers can determine whether an actuator will be able to catch a particular object, such as a spacecraft docking, a ball being caught, or a legged robot landing from a jump. In future work, we plan to apply this work to our legged robot ATRIAS (shown in Figure 8), a new legged robot, with the mechanical design detailed in [9]. When the robot takes an unexpected step down, its foot bounces, which is not a desired behavior and the robot should absorb this impact energy to stabilize the gait. We wish to know if it is possible for ATRIAS, or any legged robot that utilizes passive elements, to handle the unexpected drop-steps without bouncing, or if it is not physically possible given the actuator limitations. Using the methods described in this paper, the roboticists should be able to calculate the height of unexpected step-down that any legged robot that utilizes spring and/or damper is physically capable of handling. This will provide guidance for the researchers designing controllers, so they will know if it is possible to improve the behavior through software control.

**Figure 8.** Robot ATRIAS.



This same approach can be used to calculate the possible performance for a range of highly dynamic machines, providing insight and guidance for machine designers and control engineers alike.

## References

1. Barteit, D.; Frank, H.; Kupzog, F. Accurate Prediction of Interception Positions for Catching Thrown Objects in Production Systems. In Proceedings of the 6th IEEE International Conference on Industrial Informatics, Daejeon, Korea, 13–16 July 2008; pp. 893–898.
2. Kemper, K.; Koepf, D.; Hurst, J. Optimal Passive Dynamics for Torque/Force Control. In Proceedings of IEEE International Conference on the Robotics and Automation (ICRA), Anchorage, AK, USA, 3–8 May 2010; pp. 2149–2154.
3. Cavagna, G.A. Elastic bounce of the body. *J. Appl. Physiol.* **1970**, *29*, 279–282.
4. Full, R.J.; Farley, C.T. Musculoskeletal Dynamics in Rhythmic Systems-A Comparative Approach to Legged Locomotion. In *Biomechanics and Neural Control of Posture and Movement*; Winters, J.M., Crago, P.E., Eds.; Springer-Verlag: New York, NY, USA, 2000.
5. McMahon, T.A. The role of compliance in mammalian running gaits. *J. Exp. Biol.* **1985**, *115*, 263–282.
6. Hurst, J.W.; Rizzi, A.A. Series compliance for an efficient running gait: Lessons learned from the ECD leg. *IEEE Robot. Autom. Mag.* **2008**, *15*, 42–51.
7. Raibert, M. *Legged Robots that Balance*; MIT Press: Cambridge, MA, USA, 1986.
8. Hurst, J.W. The electric cable differential leg: A novel design approach for walking and running. *Int. J. Humanoid Robot.* **2011**, *8*, 301–321.
9. Grimes, J.; Hurst, J. The Design of ATRIAS 1.0 a Unique Monopod, Hopping Robot. In Proceedings of the International Conference on Climbing and Walking Robots (CLAWAR), Baltimore, MD, USA 23–26 July 2012.
10. An, C.; Hollerbach, J. Dynamic Stability Issues in Force Control of Manipulators. In Proceedings of IEEE International Conference on the Robotics and Automation, Raleigh, NC, 30 March–3 April 1987; Volume 4, pp. 890–896.
11. Bauml, B.; Wimbock, T.; Hirzinger, G. Kinematically Optimal Catching a Flying Ball with a Hand-Arm-System. In Proceedings of IEEE/RSJ International Conference on Intelligent Robots and Systems (IROS), Taipei, Taiwan, 18–22 October 2010; pp. 2592–2599.
12. Haddadin, S.; Albu-Schaffer, A.; de Luca, A.; Hirzinger, G. Collision Detection and Reaction: A Contribution to Safe Physical Human-Robot Interaction. In Proceedings of IEEE/RSJ International Conference on Intelligent Robots and Systems (IROS), Nice, France, 22–26 September 2008; pp. 3356–3363.
13. Schutter, J.D. A Study of Active Compliant Motion Control Methods for Rigid Manipulators Based on a Generic Control Scheme. In Proceedings of the IEEE International Conference on Robotics and Automation, Raleigh, NC, 30 March–3 April 1987; pp. 1060–1065.
14. Whitney, D.E. Force feedback control of manipulator fine motions. *J. Dyn. Syst. Meas. Control* **1977**, *99*, 91–97.
15. Haddadin, S.; Mansfeld, N.; Albu-Schaffer, A. Rigid vs. Elastic Actuation: Requirements and Performance. In Proceedings of IEEE/RSJ International Conference on Intelligent Robots and Systems (IROS), Vilamoura-Algarve, Portugal, 7–11 October 2012; pp. 5097–5104.

16. Braun, D.; Howard, M.; Vijayakumar, S. Optimal Variable Stiffness Control: Formulation and Application To Explosive Movement Tasks. *Auton. Robot.* **2012**, *33*, 237–253.
17. Garabini, M.; Passaglia, A.; Belo, F.; Salaris, P.; Bicchi, A. Optimality Principles in Stiffness Control: The VSA Kick. In Proceedings of IEEE International Conference on Robotics and Automation (ICRA), Saint Paul, MI, USA, 14–18 May 2012; pp. 3341–3346.
18. Pratt, G.A.; Williamson, M.M. Series Elastic Actuators. In Proceedings of the IEEE International Conference on Intelligent Robots and Systems, Pittsburgh, PA, USA, 5–9 August 1995; Volume 1, pp. 399–406.
19. Robinson, D.W. Design and Analysis of Series Elasticity in Closed-Loop Actuator Force Control. Ph.D. Thesis, Massachusetts Institute of Technology, Cambridge, MA, USA, June 2000.
20. Sensinger, J.; Weir, R. User-modulated impedance control of a prosthetic elbow in unconstrained, perturbed motion. *IEEE Trans. Biomed. Eng.* **2008**, *55*, 1043–1055.
21. Wyeth, G. Demonstrating the Safety and Performance of a Velocity Sourced Series Elastic Actuator. In Proceedings of IEEE International Conference on Robotics and Automation (ICRA), Pasadena, CA, USA, 19–23 May 2008; pp. 3642–3647.
22. Edsinger-Gonzales, A.; Weber, J. Domo: A Force Sensing Humanoid Robot for Manipulation Research. In Proceedings of 4th IEEE/RAS International Conference on the Humanoid Robots, Santa Monica, CA, USA, 10–12 November 2004; Volume 1, pp. 273–291.
23. Sensinger, J.; Weir, R. Improved torque fidelity in harmonic drive sensors through the union of two existing strategies. *IEEE/ASME Trans. Mechatron.* **2006**, *11*, 457–461.
24. Tsagarakis, N.; Laffranchi, M.; Vanderborght, B.; Caldwell, D. A Compact Soft Actuator Unit for Small Scale Human Friendly Robots. In Proceedings of IEEE International Conference on Robotics and Automation (ICRA), Kobe, Japan, 12–17 May 2009; pp. 4356–4362.
25. Buerger, S.; Hogan, N. Complementary stability and loop shaping for improved human ndash: Robot interaction. *IEEE Trans. Robot.* **2007**, *23*, 232–244.
26. Hurst, J.W.; Hobbelen, D.; Rizzi, A.A. Series Elastic Actuation: Potential and Pitfalls. In Proceedings of the IROS Workshop, Edmonton, Canada, 2–6 August 2005.

© 2013 by the authors; licensee MDPI, Basel, Switzerland. This article is an open access article distributed under the terms and conditions of the Creative Commons Attribution license (<http://creativecommons.org/licenses/by/3.0/>).